PERGAMON

Journal of Steroid Biochemistry & Molecular Biology 84 (2003) 181–192

The Journal of Steroid Biochemistry & Molecular Biology

www.elsevier.com/locate/jsbmb

Efficacy of Vitamin D compounds to modulate estrogen receptor negative breast cancer growth and invasion☆,☆☆

Louise Flanagan, Kathryn Packman, Brian Juba, Sharon O'Neill, Martin Tenniswood, JoEllen Welsh*

Department of Biological Sciences, University of Notre Dame, 126 Galvin Life Sciences Building, Notre Dame, IN 46556, USA

Abstract

In estrogen receptor (ER) positive breast cancer cells such as MCF-7 cells, the anti-tumor effects of $1,25(OH)_2D_3$ ($1,25D_3$) may be secondary to disruption of estrogen mediated survival signals. If so, then sensitivity to $1,25D_3$ mediated growth arrest could be reduced in estrogen independent breast cancer cells. The aim of these studies was to determine the effects of $1,25D_3$ and EB1089 on the ER negative, invasive human breast cancer cell line SUM-159PT. $1,25D_3$ and EB1089 reduced SUM-159PT cell growth subsequent to elevation of p27 and p21 levels. $1,25D_3$ mediated apoptosis of SUM-159PT cells was associated with an enrichment of membrane bound bax, a redistribution of cytochome *c* from the mitochondria to the cytosol and PARP cleavage. $1,25D_3$ and EB1089 also inhibited SUM-159PT cell invasion through an 8 μM Matrigel membrane. In pre-clinical studies, EB1089 dramatically reduced the growth of SUM-159PT xenografts in nude mice. The decreased size of tumors from EB1089 treated mice was associated with decreased proliferation and increased DNA fragmentation. Our data support the concept that Vitamin D_3 compounds trigger apoptosis by mechanisms independent of estrogen signaling. These studies indicate that Vitamin D_3 based therapeutics may be beneficial, alone or in conjunction with other agents, for the treatment of estrogen independent breast cancer.

Keywords: SUM-159PT; Hormone independent; Vitamin D; EB1089; Apoptosis; Tumor regression; Invasion

1. Introduction

1,25-Dihydroxyvitamin D_3 ($1,25D_3$), the active metabolite of Vitamin D_3, is a potent inhibitor of breast cancer cell growth via induction of growth arrest and apoptosis in vitro and in vivo [1–3]. Although the mechanisms underlying the anti-proliferative effects of $1,25D_3$ have yet to be defined, some data supports the concept that the anti-tumor effects of Vitamin D_3 compounds on ER-responsive human breast cancer cells are mediated via disruption of estrogen mediated mitogenic and survival signals [4–6]. If this is the case, then sensitivity to $1,25D_3$ mediated growth arrest/apoptosis could be reduced in estrogen independent breast cancer cells. Since late stage aggressive breast cancers with poor outcome are primarily estrogen independent, it is clearly of interest to determine whether $1,25D_3$ can induce growth arrest and/or apoptosis in estrogen independent breast cancer cells and tumors. The Vitamin D_3 receptor (VDR) is expressed in many human estrogen independent breast cancer cell lines, and $1,25D_3$ has been shown to inhibit proliferation in ER negative cell lines such as BT-20, MDA-MB-435 and MDA-MB-231, suggesting that the growth inhibitory effects of $1,25D_3$ are not solely mediated through the ER [2,7].

$1,25D_3$ inhibits cell cycle progression and induces cell death of many cancer cell lines both in vitro and in vivo [8–14]. $1,25D_3$ induced cell cycle arrest is often accompanied by up-regulation of the cyclin-dependent kinase inhibitors $p21^{Waf1}$ and $p27^{Kip1}$ and accumulation of cells in the G_1 phase of the cell cycle [6,15,16]. Analysis of G_1 regulatory proteins demonstrated that levels of CDK2, CDK4, cyclin D1 and cyclin A were decreased by $1,25D_3$ in a time dependent manner in MCF-7 cells [16,17]. These effects of $1,25D_3$ often coincide with or precede induction of apoptosis, which in MCF-7 cells results from mitochondrial disruption, bax redistribution, cytochrome *c* release and production of reactive oxygen species [18]. $1,25D_3$ mediated mitochondrial disruption is followed by downstream events including poly(ADP-ribose) polymerase (PARP) cleavage, external display of phosphatidylserine, and DNA fragmentation [18].

☆ Poster paper presented at the 15th International Symposium of the Journal of Steroid Biochemistry and Molecular Biology on "Recent Advances in Steroid Biochemistry and Molecular Biology", Munich, Germany, 17–20 May 2002.

☆☆ Portions of this work were presented at the 10th Workshop on Vitamin D, Strasbourg, France, May 1997 and the 11th Workshop on Vitamin D, Nashville, Tennessee, USA, May 2000.

* Corresponding author. Tel.: +1-574-631-3371; fax: +1-574-631-7413.
E-mail address: joellen.j.welsh.19@nd.edu (J. Welsh).

0960-0760/03/$ – see front matter © 2003 Elsevier Science Ltd. All rights reserved.
doi:10.1016/S0960-0760(03)00028-1

The inhibitory effects of $1,25D_3$ on cancer cell growth suggest that $1,25D_3$ based therapeutics may hold promise for the treatment of human cancer. Although the calcemic potency of $1,25D_3$ precludes its use as a systemic therapeutic agent, synthetic analogs of $1,25D_3$ such as EB1089 exert anti-tumor effects with minimal toxicity. In the *N*-methyl nitrosurea-induced rat mammary tumor model, EB1089 significantly inhibited tumor growth without increasing serum calcium, whereas $1,25D_3$ had no effect on tumor growth but caused hypercalcemia [13]. A phase 1 trial has evaluated the calcemic effects of EB1089 in patients with advanced cancer. EB1089 was well tolerated and its adverse effects were limited to dose dependent effects on calcium metabolism [19]. EB1089 induces regression of tumor xenografts grown in nude mice, including those derived from breast cancer (MCF-7), colon cancer (LoVo), and most recently prostate cancer [9,10,14]. Regression of EB1089 treated MCF-7 xenografts was accompanied by histological changes including characteristic apoptotic morphology and a marked reduction in the proportion of epithelial cells to stroma. These anti-tumor effects of EB1089 were evident at doses that had minimal effects on serum calcium levels [14].

The effects of Vitamin D_3 compounds on invasion, metastasis and angiogenesis of cancer cells have been less well studied. $1,25D_3$ and EB1089 reduced lung metastases in androgen insensitive metastatic prostate cancer model, and decreased the total number of bone metastases from ER-negative MDA-MB-231 cells [20,21]. $1,25D_3$ has been shown to inhibit angiogenesis in MCF-7 tumors over-expressing VEGF and the Vitamin D_3 analog 22-oxacalcitriol suppressed the growth of MDA-MB-231 cells at least partially by inhibiting neovascularization [22,23].

The consistently beneficial effects of EB1089 on proliferation, apoptosis and progression of human cancer cells prompted us to examine its efficacy against a newly characterized ER-negative invasive breast cancer cell line, SUM-159PT [24]. In these studies, we compare the effects of $1,25D_3$ and EB1089 on SUM-159PT growth, apoptosis and invasion in vitro and examine the anti-tumor efficacy of EB1089 against SUM-159PT xenografts in vivo. Our data indicate that estrogen independent, invasive cells and tumors retain responsiveness to the anti-proliferative and pro-apoptotic effects of $1,25D_3$ and EB1089. We conclude that Vitamin D_3 analogs may represent useful aternatives, either alone or in combination with other therapeutic agents, for the treatment of ER-negative, invasive breast cancers.

2. Materials and methods

2.1. Cell culture and growth assays

SUM-159PT human breast cancer cells, which were isolated from an anaplastic primary carcinoma, were obtained from the University of Michigan Breast Cancer Cell/Tissue Bank. SUM-159PT cells were cultured in Ham's F-12 medium (Life Technologies Inc., Gaithersburg, MD) containing 5 μg/ml insulin, 1 μg/ml hydrocortisone (Sigma, St. Louis, MO), and 5% charcoal-stripped serum (Hyclone, Logan, Utah). Cells were routinely passaged every 4–5 days.

For crystal violet growth assays, SUM-159PT cells were plated at a density of 4×10^3 cells/ml in media containing 5% charcoal stripped serum. Treatment with $1,25D_3$ (BIOMOL, Plymouth Meeting, PA and LEO Pharmaceuticals, Ballerup, Denmark) or EB1089 (LEO Pharmaceuticals) was initiated on the day following plating. In some experiments, cells were treated with etoposide (Calbiochem, Cambridge, MA) 2 days after plating as a positive control for apoptosis assays. In all cases, appropriate time-matched vehicle treated cells were processed in parallel. For quantitation of total adherent cell number, cells were fixed with 1% gluteraldehyde (Fisher Scientific, Pittsburgh, PA) for 15 min, incubated with 0.1% crystal violet (Fisher Scientific) for 30 min, destained with H_2O, and solubilized with 0.2% Triton X-100 (Sigma). Absorbance at 590 nm, which is proportional to total adherent cell number, was determined on a microplate reader.

2.2. $1,25(OH)_2D_3$ ligand binding assay

Cells were trypsinized, centrifuged ($500 \times g$, 5 min, 4 °C), resuspended in wash buffer (25 mM Tris pH 7.5, 250 mM sucrose, 2.5 mM $MgCl_2$, 10 mM benzamidine, 10 mM NaF, 1 mM $NaV0_4$, 10 μg/ml leupeptin, 10 μg/ml aproptinin and 1 mM PMSF) and pelleted. After supernatants were discarded, pellets were re-washed and re-pelleted. The supernatant was discarded, and the nuclear pellets were either stored at −20 °C or processed immediately. For ligand binding assay, nuclear pellets were resuspended in KTED (10 mM Tris pH 7.5, 300 mM KCl, 1 mM EDTA, 10 mM Na molybdate, 10 μg/ml leupeptin, 10 μg/ml aproptinin and 1 mM PMSF), sonicated and centrifuged (100,000 × *g*, 45 min, 4 °C) in a Beckman Optima™ ultracentrifuge (Beckman Instruments Inc., Palo Alto, CA, USA). After protein determination by the Biorad assay, proteins were precipitated and resuspended in Laemlli buffer. Binding of ^3H-$1,25(OH)_2D_3$ was determined by incubating nuclear extracts (1.5 μg/μl protein) overnight at 4 °C with increasing concentrations of ^3H-$1,25(OH)_2D_3$ (Amersham Life Science Inc., Arlington Heights, IL) in the presence or absence of excess unlabeled $1,25(OH)_2D_3$. For each sample, total binding was assayed in triplicate and non-specific binding was assayed in duplicate. Bound and free steroid were separated by incubation with dextran-coated charcoal followed by centrifugation (1500 × *g*, 20 min, 4 °C). Supernatants were removed, counted in a Beckman scintillation counter (Beckman Instruments Inc.) and data was analyzed by Scatchard plot.

2.3. Preparation of cell lysates and subcellular fractions

For cell lysates, monolayers were washed with PBS, scraped into 2 × Laemlli buffer and sonicated prior to protein

determination using the BCA protein assay. For subcellular fractionation, adherent and floating cells were pelleted by centrifugation (500 × *g*, 5 min, 4 °C), resuspended in wash buffer (25 mM Tris pH 7.5, 250 mM sucrose, 2.5 mM $MgCl_2$, 10 mM benzamidine, 10 mM NaF, 1 mM $NaVO_4$, 10 μg/ml leupeptin, 10 μg/ml aproptinin and 1 mM PMSF), pelleted (500 × *g*, 5 min, 4 °C) and resuspended in 3 vol of buffer A (20 mM HEPES-KOH 0.5 M, pH 7.5, 10 mM KCl, 1.5 mM $MgCl_2$, 1 mM EDTA, 1 mM EGTA, 250 mM sucrose, 1 mM $NaV0_4$, 25 μg/ml leupeptin, 25 μg/ml aproptinin, 2.5 μg/ml pepstatin, 1 mM PMSF, 10 mM benzamidine and 20 mM NaF), dounce homogenized, centrifuged (500 × *g*, 5 min, 4 °C) and supernatants transferred to an ultracentrifuge tube and kept on ice. The remaining pellets (containing nuclei) were resuspended in 0.5 vol of buffer A and re-centrifuged (500 × *g*, 5 min, 4 °C). The resulting pellets (nuclear fractions) were resuspended in 1.5 vol of buffer A, sonicated and analyzed for total protein. The second supernatant was combined with the supernatant from the first centrifugation and centrifuged (100,000 × *g*, 1 h, 4 °C) in a Beckman ultracentrifuge to generate the cytosolic fraction (supernatant) and the mitochondrial fraction (pellet). The pellets were resuspended in 100 μl buffer A, sonicated and analyzed for total protein.

2.4. Western blot analysis

High salt nuclear extracts, cell lysates or subcellular fractions were separated by SDS-PAGE, transferred to nitrocellulose and immunoblotted as described [18]. The antibodies used included a rat monoclonal antibody directed against VDR (clone 9A7, Neomarkers, Fremont, CA), mouse monoclonal antibodies directed against p27 (Santa Cruz, Santa Cruz, CA), p21 (Santa Cruz), cytochrome *c* (Pharmingen, San Diego, CA), cytochrome oxidase subunit II (Molecular Probes, Eugene, OR) or PARP (BIOMOL), or rabbit polyclonal antibody directed against bax (Pharmingen). Specific antibody binding was detected by appropriate horseradish peroxidase-conjugated secondary antibodies (Amersham Pharmacia Biotech, Pitcataway, NJ) and enhanced chemiluminescence (Pierce, Rockford, IL). To confirm equal loading of proteins all blots were subsequently stripped and immunoblotted with a glyceraldehyde-3-phosphate dehydrogenase (GAPDH) mouse monoclonal antibody (Biogenesis, Kingston, NH).

2.5. Electromobility shift assay

Cell pellets were resuspended in nuclear buffer (150 mM NaCl, 100 nM DTT, 5 mM $MgCl_2$, 500 nM PMSF, 1 mM EGTA pH 8.0, and 2 mM KH_2PO_4 pH 6.5) and centrifuged (800 × *g*, 2 min, 4 °C). Supernatants were removed and pellets were resuspended in nuclear buffer containing 3% Triton X-100, incubated on ice for 10 min and re-centrifuged. This procedure was repeated until complete cell lysis was achieved as determined microscopically. Final pellets were resuspended in nuclear extraction buffer (40 mM HEPES pH 7.0, 25% glycerol, 420 mM NaCl, 1.5 mM $MgCl_2$, 200 nM EDTA pH 8.0, 500 nM PMSF, and 500 nM DTT). After addition of 5 M NaCl, tubes were incubated on ice for 45 min and then centrifuged (100,000 × *g*, 45 min, 4 °C). The resulting supernatant was rapidly frozen and stored at −80 °C.

Nuclear extracts were subjected to electromobility shift assays as previously described using a Vitamin D response element (VDRE) sequence from the human *p21* gene [25]. Briefly, reactions consisted of 5 μl of labeled oligonucleotide (0.2 ng/μl), 3.5 μl of 10 × gel shift buffer, 1.0 μl poly dI:dC (1 μg/μl) (Amersham Pharmacia Biotech), 5 μl of nuclear extract (1 μg/μl) and 20.5 μl of ddH_2O. In some experiments, excess unlabeled oligonucleotide or anti-VDR antibody (Neomarkers) was included to demonstrate competition. After incubation for 30 min at room temperature, samples were electrophoresed at 150 volts for 2–3 h on a 5% non-denaturing polyacrylamide gel. The polyacrylamide gel was dried at 80 °C under vacuum, exposed to X-ray film and developed.

2.6. Matrigel invasion assay

Invasion was assessed using 8 μM Matrigel invasion chambers (Becton Dickinson, Bedford, MA). To examine the effects of $1,25D_3$ and EB1089 on invasion, two experimental designs were employed. In one, SUM-159PT cells were treated at the time of plating into the Matrigel chambers whereas in the second, cells were treated for 96 h, trypsinized and counted, and 25,000 cells were plated into the chambers. In both designs, the number of invasive cells was determined 96 h later. Cells that invaded the 8 μM Matrigel membrane and attached to the bottom of the well were trypsinized and counted.

2.7. Nude mouse xenograft model

Six-week-old ovariectomized female NCr-*nu* mice (Taconic Farms, Germantown, NY), were used as hosts for SUM-159PT xenografts. Mice were fed a low calcium (0.1%) diet upon arrival and for the duration of the study to minimize the calcemic effects of EB1089. Mice were inoculated with SUM-159PT cells either subcutaneously or orthotopically into the mammary fat pad. SUM-159PT cells were trypsinized, pelleted and resuspended in Matrigel/Ham's F-12 media (4:1). Mice were injected subcutaneously with 5×10^6 cells/0.3 ml on the lateral flank, or orthotopically with 1×10^6 cells/0.1 ml injection directly into the mammary fat pad under anesthesia (50 mg/kg of pentobarbital). Body weight and tumor size was monitored weekly by caliper measurements of the length, width and height, and volume was calculated using the formula for a semi-ellipsoid ($4/3\pi r^3/2$). When tumor volume reached approximately 200 mm^3 (3–4 weeks), mice were randomized to control or EB1089 treatment groups. Administration of EB1089 was either by daily subcutaneous injection (45 pmol EB1089 in propylene

glycol/PBS, 4:1) or via implanted continuous release pellets designed to deliver either 60 or 120 pmol EB1089 per day (custom made by Innovative Research of America, Sarasota, FL). Control animals received either daily vehicle injections or placebo pellets. After 4–5 weeks of treatment, mice were euthanized, blood was collected by cardiac puncture, and tumors and organs were removed, examined and fixed in 4% formalin (Fisher Scientific) for histological analysis.

2.8. Histological analysis of tumors and organs

For routine morphological assessment, tumors were embedded in paraffin, sectioned at 5 μm and stained with hematoxylin (Gill's formulation 3, Fisher Scientific) and eosin Y (Sigma). Mitotic and apoptotic cells were identified by immunohistochemistry for proliferating cell nuclear antigen (PCNA) and by the TUNEL assay. For PCNA, sections were incubated with mouse monoclonal anti-PCNA (Nova Castra Laboratories, Newcastle Upon Tyne, UK) at a 1:50 dilution in 1% BSA-PBS. The secondary biotin conjugated antibody (Vector Laboratories, Burlingame, CA) was applied at a 1:200 dilution in 1% BSA-PBS. The ABC technique followed by diaminobenzidine was used to localize peroxidase, and sections were counterstained with hematoxylin (Harris modified, Fisher). TUNEL was performed with a commercially available assay according to manufacturer's directions (Boehringer Mannheim, Indianapolis, IN).

3. Results

3.1. Vitamin D_3 receptor expression and function in SUM-159PT cells

To determine whether SUM-159PT cells had the potential to respond to Vitamin D_3 compounds, we first examined the expression of the VDR. Western blot analysis of nuclear extracts indicated that basal expression of the VDR in control (ethanol treated) SUM-159PT cells was barely detectable (Fig. 1A). After treatment with 100 nM $1,25D_3$ or 100 nM EB1089 for 48 or 96 h, however, characteristic homologous up-regulation of the VDR was observed. To determine if the VDR expressed in SUM-159PT cells was capable of binding ligand, ^{3}H-$1,25D_3$ binding assays were performed and analyzed by Scatchard plot (Fig. 1B). The data indicate that nuclear extracts from SUM-159PT cells exhibited specific, saturable $1,25D_3$ binding, with a Bmax of 8.9 fmol/mg protein and a K_d value of 3×10^{-11} M.

To test if the VDR expressed in SUM-159PT cells was capable of binding sequence specific DNA, electromobility

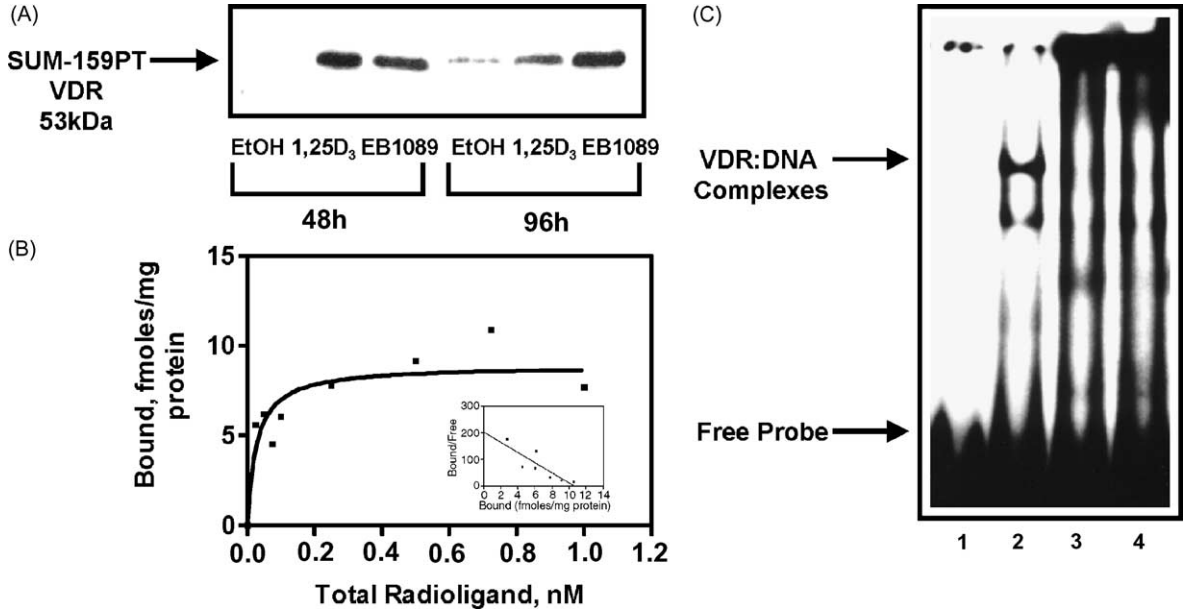

Fig. 1. VDR function studies. (A) Western blot analysis of VDR expression in SUM-159PT cells and the effects of $1,25D_3$ on its protein expression. Nuclear extracts prepared from SUM-159PT cells treated with ethanol vehicle, 100 nM $1,25D_3$ or 100 nM EB1089 for the indicated times, were separated on 10% SDS-PAGE gels and immunoblotted with a rat monoclonal antibody directed against the human VDR. Blots are representative of three independent experiments. (B) Scatchard analysis of the VDR in SUM-159PT cells. Nuclear extracts derived from untreated SUM-159PT cells were used for ligand binding assays over a range of ^{3}H-$1,25D_3$ concentrations (0.01–1 nM). Data are expressed as femtamoles of $1,25D_3$ specifically bound per mg nuclear extract protein after subtraction of non-specific binding. The Bmax of the VDR in SUM-159PT cells was determined to be 8.9 fmol/mg bound protein. The K_d value or the affinity of the VDR for $1,25D_3$ was determined to be 3×10^{-11} M. The data is representative of two independent trials with each data point assayed in triplicate. (C) EMSA analysis of the VDR in SUM-159PT cells using the p21 VDRE. Arrows indicate the VDR:DNA complexes and the free probe: lane 1, labeled p21 VDRE probe; lane 2, SUM-159PT nuclear extracts plus labeled p21 VDRE probe; lane 3, SUM-159PT nuclear extracts, labeled p21 VDRE probe plus 50× cold p21 VDRE; lane 4, SUM-159PT nuclear extracts, labeled p21 VDRE probe plus Vitamin D monoclonal antibody. Data is representative of at least three independent experiments.

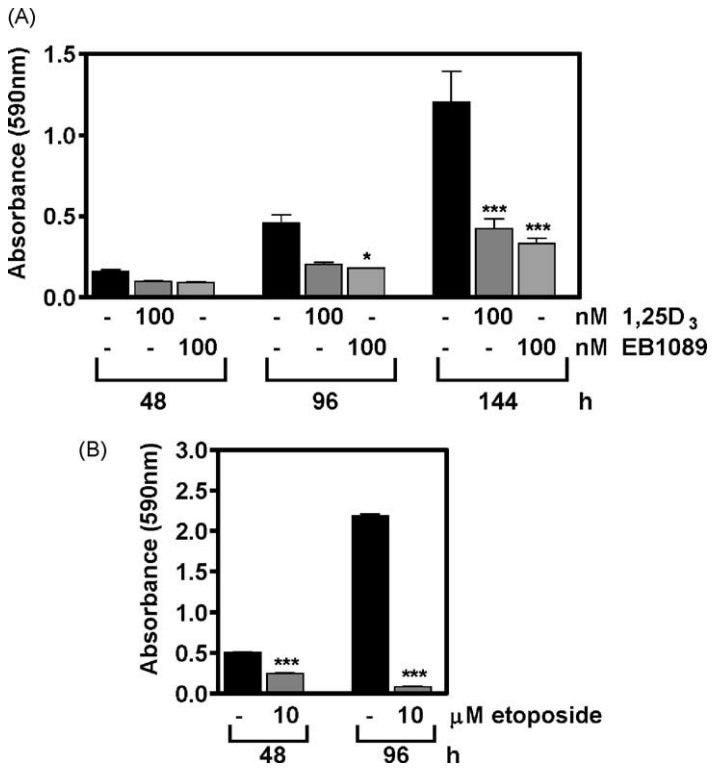

Fig. 2. Effects of $1,25D_3$, EB1089 or etoposide on proliferation of SUM-159PT cells. (A) On the day following plating, cells were treated with ethanol vehicle (-), 100 nM $1,25D_3$ or 100 nM EB1089 for the indicated times. (B) Two days following plating, cells were treated with ethanol vehicle (-) or 10 μM etoposide for the indicated times. For all treatments total cell number was determined by crystal violet staining. Data represents mean ± S.E.M. of four values per time point. Similar results were obtained from at least two other independent experiments: $^{***}P < 0.001$; ethanol control vs. treated.

shift assays were performed with an oligonucleotide sequence designed to mimic the Vitamin D response element (VDRE) found in the human p21 promoter (Fig. 1C). Two distinct retarded bands were identified when SUM-159PT nuclear extracts were incubated with the p21 VDRE sequence (lane 2), whereas no bands were detected in the absence of nuclear protein (lane 1). Similar results were obtained with oligonucleotide sequences modeled after VDREs from the parathyroid hormone (PTH) VDRE (data not shown). The specificity of these interactions was demonstrated by inclusion of excess unlabeled VDRE sequence in the reaction, which competed away both bands (lane 3). The presence of the VDR in these complexes was demonstrated by inclusion of VDR antibody during the reaction, which also competed away both bands (lane 4).

3.2. Effects of Vitamin D_3 compounds on SUM-159PT cells in vitro

Having demonstrated the presence of the VDR in SUM-159PT cells, we next compared the effects of $1,25D_3$ and EB1089 on cell growth with that of etoposide, an established chemotherapeutic drug that induces apoptosis via inhibition of topoisomerase II. SUM-159PT cells were treated with 100 nM $1,25D_3$, 100 nM EB1089 or ethanol vehicle, and adherent cell number was assessed after 2, 4 and 6 days. As indicated in Fig. 2A, treatment with either $1,25D_3$ or EB1089 significantly reduced SUM-159PT cell number within 2 days, and induced a 60–70% reduction in cell number relative to that of control after 6 days. Treatment of SUM-159PT with 10 μM etoposide caused a rapid and more dramatic reduction in cell number than either Vitamin D_3 compound (50% of control within 48 h). After 96 h, cell numbers in etoposide treated cultures were only 3% of that in control cultures (Fig. 2B).

Because previous work has demonstrated that breast cancer cells treated with $1,25D_3$ exhibit cell cycle arrest [16], we examined the expression of p21 and p27 (inhibitors of G_1 to S phase progression) and the $cdc2^{p34}$ kinase (required for M phase progression). As demonstrated in Fig. 3, treatment of SUM-159PT cells with 100 nM $1,25D_3$ or 100 nM EB1089 increased both p27 and p21 expression relative to time matched vehicle control cells within 48 h. In contrast, EB1089 but not $1,25D_3$ down-regulated expression of the $cdc2^{p34}$ kinase after 72 h (Fig. 3).

We next assessed whether $1,25D_3$ or EB1089 had the ability to induce SUM-159PT cell death in vitro. In cultures treated with $1,25D_3$ or EB1089, typical apoptotic morphology was evident (condensed, irregularly shaped nuclei, and positive TUNEL staining) within 72 h (data not shown). To further elucidate the apoptotic pathway in the SUM-159PT cells we analyzed the expression and subcellular distribution

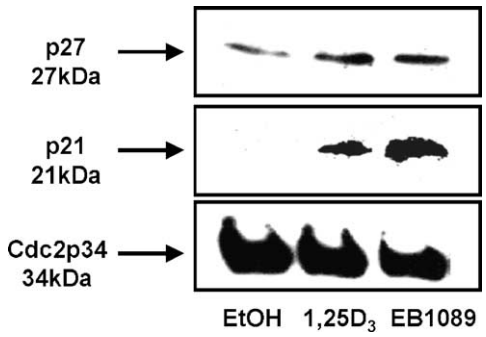

Fig. 3. Expression of cell cycle related proteins in SUM-159PT cells after treatment with $1,25D_3$ and EB1089. Cell lysates prepared from SUM-159PT cells treated with ethanol vehicle, 100 nM $1,25D_3$ or 100 nM EB1089 for 48 h were separated on 12.5% SDS-PAGE gels and immunoblotted with mouse monoclonal antibodies directed against p27, p21 and $cdc2^{p34}$. Blots are representative of two independent experiments.

of several proteins that have been linked to $1,25D_3$ mediated apoptosis in MCF-7 cells [26]. $1,25D_3$ or EB1089 treatment of SUM-159PT cells induced subcellular redistribution of the pro-apoptotic protein bax, similar to MCF-7 cells (data not shown), indicative of translocation that has been functionally linked to transmission of the apoptotic signal [27]. Translocation of bax was associated with reduced mitochondrial cytochrome *c* and increased cytosolic cytochrome *c* after 96 h treatment with $1,25D_3$ or 48 h treatment with etoposide (Fig. 4A). To exclude mitochondrial contamination in the cytosol fractions, cytochrome oxidase expression was assessed and found to be present only in the mitochondrial fractions (data not shown).

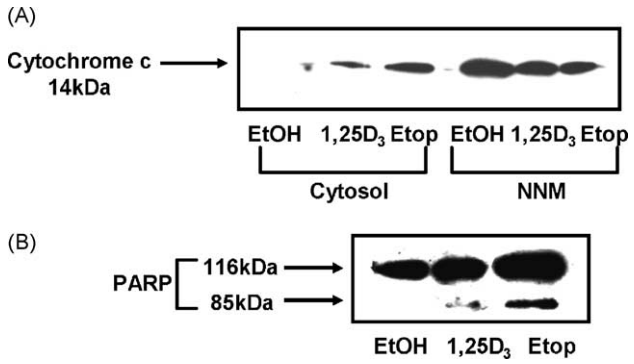

Fig. 4. Expression of apoptosis related proteins in SUM-159PT cells after treatment with $1,25D_3$ and etoposide. (A) Subcellular distribution of cytochrome *c* after treatment with $1,25D_3$ and etoposide. Cytosol and non-nuclear membrane (NNM) fractions prepared from SUM-159PT cells treated with ethanol vehicle, 100 nM $1,25D_3$ for 96 h or 10 μM etoposide for 48 h were separated on 12.5% SDS-PAGE gels and immunoblotted with a mouse monoclonal antibody directed against cytochrome *c*. Blots are representative of two independent experiments. (B) Effects of $1,25D_3$ and etoposide on PARP cleavage. Nuclear fractions prepared from SUM-159PT cells treated with ethanol vehicle, 100 nM $1,25D_3$ for 96 h or 10 μM etoposide for 48 h were separated on a 7.5% SDS-PAGE gel and immunoblotted with a mouse monoclonal antibody directed against PARP. Blot is representative of two independent experiments.

To determine whether caspase activation was involved in apoptosis of SUM-159PT cells, we assessed the cleavage of PARP, a substrate of caspases-3 and -7. SUM-159PT cells treated with 100 nM $1,25D_3$ for 96 h or 10 μM etoposide for 48 h were analyzed by immunoblotting with an antibody that recognizes both intact PARP (116 kDa) and the apoptotic cleavage product (85 kDa). In extracts from SUM-159PT cells treated with $1,25D_3$ or etoposide, the 85 kDa PARP cleavage fragment was detected, whereas no PARP cleavage was detected in EtOH treated control cells (Fig. 4B).

3.3. Effect of EB1089 on growth of SUM-159PT tumors in vivo

To determine whether the Vitamin D analog EB1089 could modulate growth and/or apoptosis of SUM-159PT tumors in vivo, we utilized ovariectomized nude mice bearing SUM-159PT xenografts at both subcutaneous and orthotopic (mammary fat pad) sites. For both approaches, mice were implanted with drug delivery pellets designed to continuously release 60 or 120 pmol EB1089 per day. The impact of EB1089 pellets on growth of subcutaneous SUM-159PT tumors is presented in Fig. 5A. The average tumor volume increased rapidly in control mice implanted with placebo pellets over the 4 week period. In mice implanted with EB1089 pellets, average tumor volume decreased gradually over the 4 weeks of treatment. Tumor volume after 4 weeks was significantly ($P < 0.001$) lower in the EB1089 treated groups ($70.3 \pm 39.4\,mm^3$ for 60 pmol EB1089 group, $n = 6$; $99.7 \pm 61.3\,mm^3$ for the 120 pmol EB1089 group, $n = 4$) than in the control group ($656.5 \pm 321.05\,mm^3$, $n = 10$). In addition, although not evident from the graph (which shows mean tumor volume), two SUM-159PT tumors completely regressed in response to EB1089 treatment. In this same study, additional groups of nude mice bearing SUM-159PT tumors were injected daily with either vehicle or 45 pmol EB1089, but no differences were observed between EB1089 and vehicle treated (data not shown). As an indication of potential calcemic side effects of Vitamin D analog treatment, we assessed serum calcium levels in tumor bearing mice. Serum calcium in mice implanted with EB1089 pellets (11.48 ± 0.5 mg/dl for 60 pmol EB1089; 11.8 ± 0.6 mg/dl for 120 pmol EB1089) was not significantly elevated compared to mice implanted with placebo pellets (10.81 ± 0.6 mg/dl). In contrast, tumor bearing mice treated with daily injections at the lower dose of 45 pmol EB1089 daily exhibited elevated serum calcium levels (13.27 ± 0.8 mg/dl) after 4 weeks of treatment despite been maintained on the low calcium diet. These data suggest that pellet delivery may alleviate or minimize the calcemic side effects of Vitamin D_3 based therapeutics.

In our second in vivo study, the growth kinetics of SUM-159PT tumors maintained in the mammary fat pad were measured in ovariectomized nude mice using a design similar to the first study. The doubling time for SUM-159PT tumors growing in the mammary fat pad was calculated to

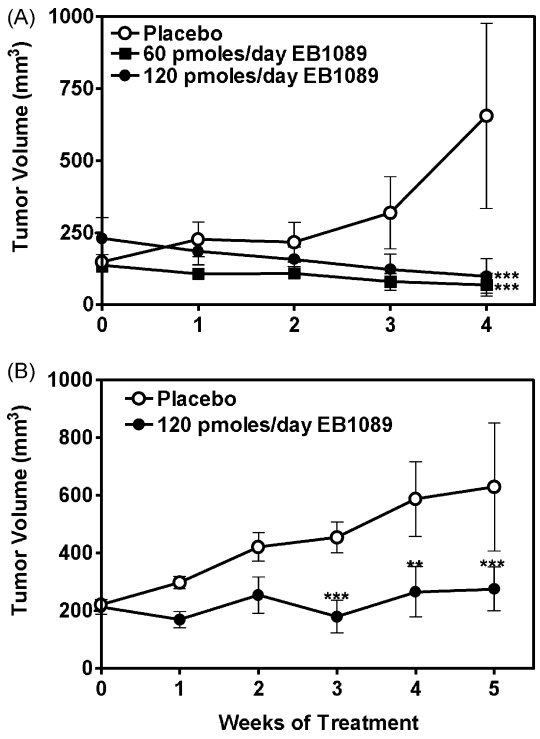

Fig. 5. Effects of EB1089 on the volume of SUM-159PT tumors. (A) Ovariectomized nude mice bearing subcutaneous tumors were surgically implanted with either a placebo pellet or continuous slow release pellets designed to release 60 or 120 pmol EB1089 per day. Tumor volumes were monitored weekly and calculated as described in Section 2. Each point represents the mean ± S.E.M. of 10 control mice, six 60 pmol EB1089 treated mice and four 120 pmol EB1089 treated mice: $^{***}P < 0.001$. (B) Ovariectomized nude mice bearing tumors in the mammary fat pad were surgically implanted with either placebo pellets or continuous slow release pellets designed to release 120 pmol EB1089 per day. Tumor volumes were monitored weekly and calculated as described in Section 2. Each point represents the mean ± S.E.M. of 22 control mice, and eighteen 120 pmol EB1089 treated mice: $^{**}P < 0.01$; $^{***}P < 0.001$.

be 27 ± 7.5 days, which is comparable to that observed in a rapidly growing human breast tumor. The growth kinetics of the SUM-159PT tumors inoculated subcutaneously were similar to those grown orthotopically, although a higher initial cell count per injection was required for successful tumor development at subcutaneous sites (see Section 2).

The impact of EB1089 treatment on SUM-159PT tumors growing in the mammary fat pad is depicted in Fig. 5B. In control mice, average tumor volume increased over the 5 week treatment period. In EB1089 treated mice, tumor volumes decreased gradually over the 5 weeks of treatment. Tumor volume after 5 weeks was significantly ($P < 0.001$) lower in the EB1089 treated groups (275.8 ± 75.9 mm^3, $n = 18$) than in the control group (629.7 ± 227.7 mm^3, $n = 22$). This indicates that the effects of EB1089 on SUM-159PT tumors grown orthotopically are similar to those observed for SUM-159PT tumors inoculated subcutaneously.

3.4. Effect of EB1089 on morphology, proliferation and apoptosis of SUM-159PT tumors

Sections from SUM-159PT tumors stained with hematoxylin and eosin for assessment of general morphology are presented in Fig. 6A and B. SUM-159PT tumors growing in the mammary fat pad were composed of solid sheets of epithelial tumor cells with little intervening mouse stroma and frequent blood vessels (Fig. 6A). The majority of the epithelial cells were quiescent, although mitotic figures were usually visible in each section. In many tumors, abnormal cruciform mitotic figures were observed, indicating an aggressive undifferentiated growth pattern (Fig. 6B).

Representative photos of SUM-159PT tumor sections from mice treated with placebo or 120 pmol per day EB1089 for 5 weeks and stained with hematoxylin and eosin for assessment of general morphology are presented in Fig. 6C and D. Tumors from placebo treated mice were primarily composed of tightly packed epithelial cells, with small amounts of mouse-derived stoma (Fig. 6C). In contrast, tumors from mice treated with 120 pmol per day EB1089 displayed an increased percentage of stroma and loss of epithelial cells (Fig. 6D). Mitotic figures were readily identified in control tumors and few cells with apoptotic morphology were observed. In contrast, EB1089 tumors were composed of quiescent epithelial cells with few mitotic figures visible. In many areas, epithelial cells with classic apoptotic morphology (condensed cells with pyknotic nuclei) were frequent. Treatment of mice bearing subcutaneous SUM-159PT tumors with EB1089 induced similar morphology as that described for orthotopic tumors.

To determine whether the changes in SUM-159PT tumor morphology induced by EB1089 were associated with alterations in mitotic or apoptotic index, we examined expression of PCNA (as a marker of proliferation) and DNA fragmentation (as a marker of apoptosis). In control tumors, PCNA expression was detected in the nucleus of approximately 60% of all epithelial cells, but in particular its expression was localized at the periphery of the tumor where the cells were most actively growing (Fig. 7A). In many tumors, especially the rapidly growing control tumors, little or no proliferation was observed in the central region of the tumor. A decrease in PCNA expression (approximately 30% expression) was detected in tumors from mice treated with EB1089 for 5 weeks (Fig. 7B). The staining pattern of PCNA was more uniform throughout the entire EB1089-treated tumor as compared to control tumors, due perhaps to smaller and more slower growing tumors after EB1089 treatment.

Assessment of TUNEL positive cells was used to detect DNA fragmentation as a marker of apoptosis in SUM-159PT tumor sections derived from control and EB1089 treated mice. In control tumors, TUNEL expression was detected in the nucleus of approximately 20% of all epithelial cells, but in particular its expression too was localized at the periphery of the tumor where the greatest amount of epithelial cell turnover was occurring (Fig. 7C). Sections of tumors from

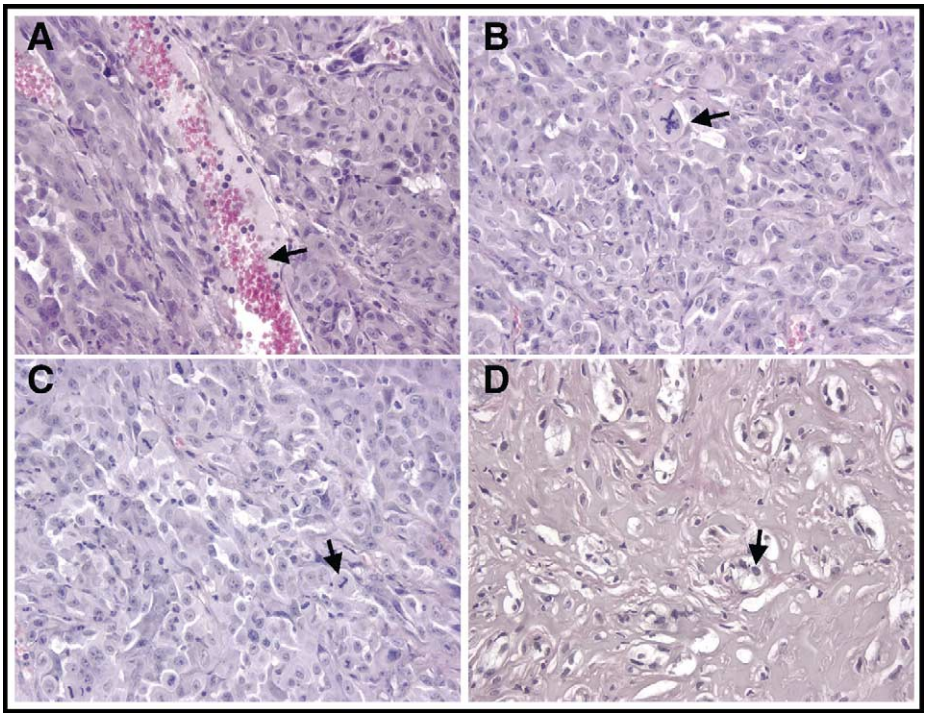

Fig. 6. Morphology of SUM-159PT tumors. Representative tumor sections from untreated mice were formalin fixed, paraffin embedded, sectioned, and stained with hematoxylin and eosin (A and B). Arrow indicates (A) vascularization in SUM-159PT tumors; (B) cruciform mitotic figure. Representative tumor sections from mice treated with placebo or 120 pmol per day EB1089 pellets for 5 weeks were stained with hematoxylin and eosin (C and D). Arrow indicates (C) mitotic figure in control tumor; (D) apoptotic cells in EB1089 tumor. Photographed at 40× magnification.

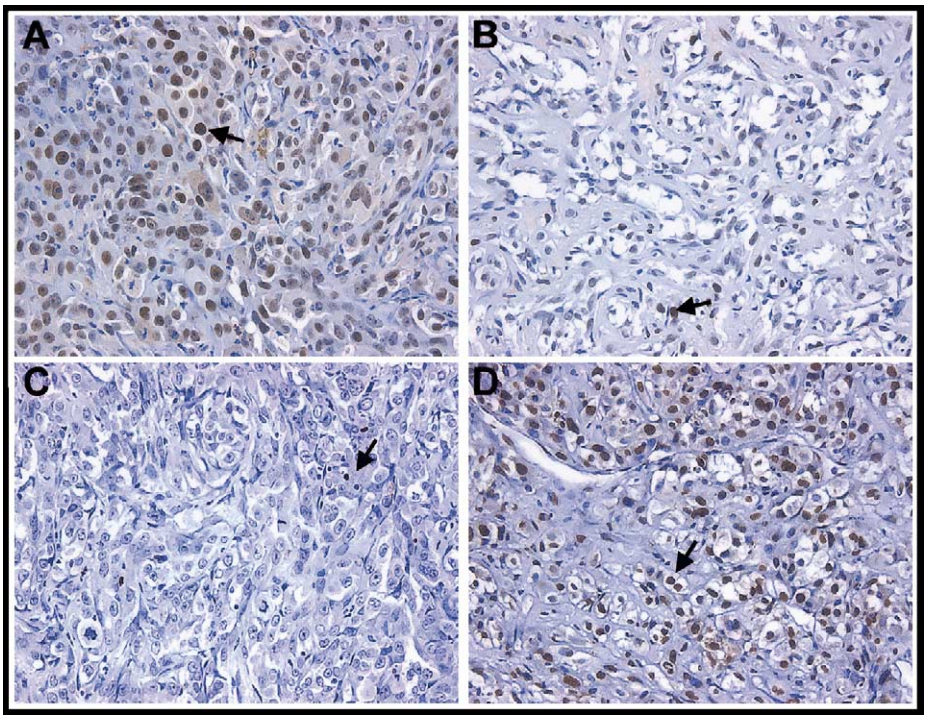

Fig. 7. Effect of EB1089 treatment on PCNA expression and DNA fragmentation in SUM-159PT tumors. Expression of PCNA in representative tumor sections from mice treated with (A) placebo or (B) 120 pmol per day EB1089 pellets for 5 weeks. Sections were incubated with a mouse monoclonal antibody directed against human PCNA and visualized with DAB (brown nuclear staining indicated by arrows). Representative tumor sections from mice treated with (C) placebo or (D) 120 pmol per day EB1089 pellets for 5 weeks were processed for TUNEL. Arrows indicate TUNEL positive cells (brown nuclear staining). Photographed at 40× magnification.

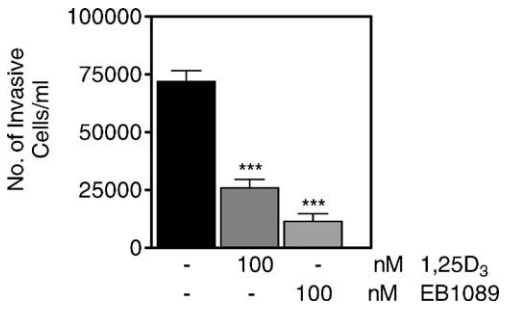

Fig. 8. Effects of $1,25D_3$ or EB1089 on SUM-159PT invasion in vitro. SUM-159PT cells treated with EtOH (-), 100 nM $1,25D_3$ or 100 nM EB1089 were analyzed in the Boyden chamber invasion assay. Cells that invaded the 8 μM Matrigel membrane and attached to the bottom of the well were trypsinized and counted. The data represent the mean ± S.E.M. from three wells. These data are representative of two independent experiments.

EB1089 treated mice showed an overall increased number of TUNEL positive cells with approximately 60% of the epithelial cells staining positively for TUNEL (Fig. 7D).

3.5. Effects of Vitamin D_3 compounds on invasion of SUM-159PT cells

We have previously reported that SUM-159PT cells are capable of local invasion and metastasis in vivo and are positive in in vitro invasion assays [24]. To test whether $1,25D_3$ or EB1089 could directly modulate invasion of SUM-159PT cells, we used the Boyden chamber invasion assay. SUM-159PT cells plated on Matrigel were treated with vehicle, 100 nM $1,25D_3$ or 100 nM EB1089 for 96 h and invasion was quantitated. As depicted in Fig. 8, $1,25D_3$ treatment reduced the number of invasive cells by 65% and EB1089 treatment was even more effective (80% reduction). Similar results were observed when SUM-159PT cells were treated for 96 h with $1,25D_3$ or EB1089 prior to plating on Matrigel membranes, thereby eliminating the possibility that the reduction in invasive cells solely reflected a decrease in cell number (data not shown).

4. Discussion

In these studies, we demonstrate that SUM-159PT cells, a highly anaplastic, invasive and metastatic cell line derived from an ER negative primary human breast tumor, expresses the VDR and is responsive to the growth inhibitory effects of $1,25D_3$ and its analog EB1089 both in vitro and in vivo. The presence of the VDR in breast cancer cells was demonstrated in human biopsies, and has since been found in many breast cancer cell lines as well as normal breast [28]. Although the basal expression of VDR is low in SUM-159PT cells, both $1,25D_3$ and EB1089 up-regulate VDR levels. This up-regulation has been attributed to stabilization of the receptor by ligand binding in other in vitro systems [29]. In agreement with this concept, we propose that homologous VDR up-regulation in SUM-159PT cells is also due to protein stabilization, as previous studies have demonstrated that $1,25(OH)_2D_3$ did not up-regulate VDR promoter activity in SUM-159PT cells [30].

Although a functional VDR is a prerequisite for a growth regulatory response to $1,25D_3$, the presence of the VDR is not sufficient for growth-inhibition in response to $1,25(OH)_2D_3$. For example, MCF-7 cells selected for resistance to $1,25D_3$ express VDR which is capable of binding $1,25D_3$ and specific VDREs, however, these cells do not respond to the growth-inhibitory effects of $1,25D_3$ [25]. In SUM-159PT cells, VDR expression was demonstrated by western blot, and VDR function was established by $1,25D_3$ binding studies and electrophoretic gel shift assays. While $1,25D_3$ binding in SUM-159PT cells was less than that previously observed in MCF-7 cells, it was comparable to that observed in the ER-negative MDA-MB-231 cell line (2.9 fmol/mg) [28]. Furthermore, a significant growth inhibitory effect of $1,25D_3$ was observed in SUM-159PT cells, conclusively demonstrating that the VDR pathway in SUM-159PT cells is functional.

In ER-positive breast cancer cells, the effects of $1,25D_3$ are similar to those induced by anti-estrogens, and $1,25D_3$ transcriptionally down-regulates ER expression [31,32]. These findings have suggested that, at least in MCF-7 cells, the effects of $1,25D_3$ may be related to disruption of estrogen mediated survival signals. If so, then sensitivity to $1,25D_3$ mediated growth arrest and apoptosis could be reduced in estrogen independent breast cancer cells. However, our results indicate that $1,25D_3$ inhibits proliferation and induces apoptosis in the ER-independent SUM-159PT cells, thus, while disruption of ER signaling may contribute to the effects of $1,25D_3$ in estrogen dependent breast cancer cells, these effects are not dependent upon estradiol signaling. This conclusion is consistent with our finding that the mechanism by which $1,25D_3$ and EB1089 reduce growth of SUM-159PT cultures appears to be similar to that of ER positive cells [6,16]. Both Vitamin D compounds induce cell cycle arrest in G_0/G_1 in association with up-regulation of p21 and p27 and down-regulation of $cdc2^{p34}$. Furthermore, like MCF-7 cells, SUM-159PT cells undergo $1,25D_3$ mediated apoptosis via redistribution of bax from cytosol to non-nuclear membranes and release of cytochrome *c* from the mitcohondria. In addition, activation of downstream caspases in response to Vitamin D compounds was suggested by the observation that PARP, a caspase substrate, was cleaved in SUM-159PT treated with $1,25D_3$. These are the first studies to describe intracellular signaling events leading to apoptosis in ER-negative breast cancer cells. SUM-159PT cells thus provide a model system for characterization of the mechanism by which VDR triggers bax redistribution, and for identification of the specific caspases that are activated during $1,25D_3$ mediated apoptosis.

Another goal of our studies was to determine if Vitamin D mediated growth inhibition was of sufficient magnitude to

impact on the growth of invasive and metastatic ER-negative cells in vivo. In a series of nude mice studies, we demonstrated that EB1089 significantly reduced the growth of established SUM-159PT tumors. Xenografts grown as subcutaneous implants in ovariectomized nude mice treated with EB1089 were approximately 85% smaller than those of placebo treated mice. When injected orthotopically into the mammary fat pad, SUM-159PT cells formed tumors which were invasive and metastatic, and EB1089 inhibited growth of these tumors by 65–70%. The number of secondary tumors was also reduced in EB1089 treated mice, however, it is unclear whether this represents a direct effect of EB1089 on metastatic potential, or an indirect effect due to the smaller size of the primary tumors. An inhibitory effect of EB1089 on metastasis in vivo is consistent with our in vitro invasion assays which demonstrated that $1,25D_3$ and EB1089 reduce invasion of SUM-159PT cells independent of their anti-proliferative effects. This data complements a previous report that $1,25D_3$ inhibited invasion of ER-negative MDA-MB-231 breast cancer cells [33]. Further investigation on the molecular mechanisms by which EB1089 prevents SUM-159PT invasion and metastasis would clearly be of interest.

The results of our study are in agreement with previous work that demonstrated anti-tumor effects of the Vitamin D analog 22-oxacalcitriol when injected into tumors beginning 4 days after transplantation. At the most effective dose (1 μg/kg body weight), 22-oxacalcitriol reduced final tumor weight by 70% [8]. In a follow up study, oral administration of 22-oxacalcitriol three times weekly also significantly reduced the growth of MX-1 tumors. Because of the short time between tumor transplantation and initiation of 22-oxacalcitriol treatment however, these studies did not discriminate effects of the Vitamin D analog on initial tumor take from those on tumor growth kinetics [34]. In contrast, our experimental design was specifically designed to test the effectiveness of EB1089 against established, rapidly growing tumors, and as such represents the first report on the effectiveness of a Vitamin D analog against established estrogen independent breast tumors. This data is complementary to previous studies that demonstrated effectiveness of EB1089 in inhibiting growth of established tumors induced in rats with *N*-methyl nitrosurea or established ER positive MCF-7 xenografts [35,14].

With higher doses of EB1089 more effective tumor regression was seen however serum calcium levels rose [35]. In our nude mice bearing subcutaneous tumors, daily injections of 45 pmol per day EB1089 had no effect on tumor volume but did cause hypercalcemia. This may be specific for this route of administration, since nude mice were able to tolerate higher doses with pellet delivery of EB1089 without hypercalcemia. These results suggest that at least in this model system, administration of EB1089 by continuous release may minimize the side effects of Vitamin D analogs and maximize the induction of tumor regression.

This aggressive tumor biology is consistent with the expression of metastatic markers and in vitro invasiveness in SUM-159PT cells. Metastases were observed in the lymph nodes, muscle area surrounding the mammary fat pad, lungs and liver, consistent with previous reports of metastatic sites after inoculation of other breast cancer cells into the mammary fat pad of nude mice [36]. Metastatic spread was not observed when SUM-159PT cells were inoculated subcutaneously. Therefore, implantation of tumor cells into anatomically appropriate (orthotopic) sites, rather than subcutaneously, allowed for the metastatic potential of SUM-159PT cells. The present work correlates with the work of many other groups which indicate that the mammary fat pad is a more favorable site than the subcutis for the generation of metastases of mammary tumors [36,37].

Histological examination of SUM-159PT primary tumors indicated an undifferentiated, aggressive phenotype with abnormal mitotic figures and high levels of vascularization. Histological analysis indicated that the decreased size of the tumors from EB1089-treated mice, compared with that in control mice, was associated with a reduction in the epithelial component and an increase in the stroma. The reduction of tumor volume in mice treated with 120 pmol per day EB1089 for 5 weeks could reflect a decreased rate of cell proliferation or an increased rate of cell death or both. Our analyses confirmed that EB1089 mediates tumor regression by modulation of both apoptosis and proliferation of tumor epithelial cells. Tumors from EB1089 treated mice exhibited apoptotic morphology and a high proportion of TUNEL-positive cells compared with tumors from control mice. Our data demonstrating apoptosis in EB1089 treated SUM-159PT tumors is consistent with data from EB1089 treated MCF-7 xenografts, and also correlates with our data that $1,25(OH)_2D_3$ and EB1089 induce apoptosis in SUM-159PT cells in vitro [14]. An effect of EB1089 on tumor cell apoptosis is also supported by our observation that some EB1089 treated tumors completely regressed. In addition to induction of apoptosis, EB1089-treated tumors exhibited a decrease in proliferation after 5 weeks of treatment, as measured by PCNA. These data are again consistent with in vitro work indicative that $1,25D_3$ and EB1089 increase levels of p21 and p27, thereby inducing a block in the cell cycle, in many breast cancer cell lines.

In summary our work, combined with previously published work, emphasizes that Vitamin D compounds and anti-estrogens such as tamoxifen regulate growth and apoptosis of breast cancer cells by independent mechanisms. Analyses of human breast cancer tumor biopsies have demonstrated that the VDR and ER do not necessarily co-localize within the same cell, indicating that these two nuclear receptors are present in distinct target cells within a mixed tumor [38]. This suggests that in cells expressing both ER and VDR, $1,25D_3$ through the VDR, actively induces growth arrest and facilitates apoptosis, whereas treatment with anti-estrogens disrupts ER signaling, disrupting the mitogenic effects of estrogen. In estrogen independent

cells, the estrogen signaling pathway is disrupted, allowing for the escape from estrogen dependence and resistance to anti-estrogen mediated apoptosis. However, the presence of the VDR in anti-estrogen resistant cells renders them sensitive to activation of apoptosis in response to $1,25D_3$. This therefore suggests that for patients with breast tumors containing estrogen dependent and estrogen independent cells, a distinct therapeutic advantage may be achieved by combining therapies that activate VDR with those that disrupt estrogen signaling. Vitamin D analogs may offer an effective therapeutic approach for aggressive, late stage tumors that exhibit resistance to the standard anti-estrogen regimens. Our data are the first to show apoptotic established tumor regression of an ER-independent breast cancer model system by the Vitamin D analog EB1089 and are consistent with previous reports of tumor regression and apoptosis in the ER-dependent MCF-7 tumors [14]. Our work also shows that sensitivity of breast tumors to the Vitamin D analog EB1089 is not diminished in tumors which have progressed to estrogen independence.

To summarize, the VDR is present in both estrogen-dependent and estrogen-independent breast cancer cell lines and sensitivity to Vitamin D compounds is not diminished or lost in breast cancer cells that have progressed to estrogen independence. Pre-clinical animal studies demonstrate significant effects on the growth of estrogen-independent tumors, indicating that Vitamin D compounds trigger growth arrest and apoptosis by a mechanism that is independent of an estrogen-regulated pathway.

Acknowledgements

This work was supported by an Army Breast Cancer Research Program Grant to Louise Flanagan (DAMD17-99-1-9337), an AICR award (98A100) and an NIH award (CA69700) to JoEllen Welsh. We would like to thank Dr. Steve Ethier (University of Michigan Cell/Tissue Bank) for the SUM-159PT cells. We thank Carol Spierto, Pamela Murphy and Kenneth Jones for assistance with the animal studies. We would also like to thank Dr. Ian Byrne for technical assistance.

References

[1] J. Welsh, Induction of apoptosis in breast cancer cells in response to Vitamin D and antiestrogens, Biochem. Cell Biol. 72 (11–12) (1994) 537–545.

[2] R.S. Fife, G.W. Sledge Jr., C. Proctor, Effects of Vitamin D_3 on proliferation of cancer cells in vitro, Cancer Lett. 120 (1) (1997) 65–69.

[3] M. Simboli-Campbell, C.J. Narvaez, M. Tenniswood, J. Welsh, 1,25-Dihydroxyvitamin D_3 induces morphological and biochemical markers of apoptosis in MCF-7 breast cancer cells, J. Steroid Biochem. Mol. Biol. 58 (4) (1996) 367–376.

[4] A. Stoica, M. Saceda, A. Fakhro, H.B. Solomon, B.D. Fenster, M.B. Martin, Regulation of estrogen receptor-alpha gene expression by 1,25-dihydroxyvitamin D in MCF-7 cells, J. Cell Biochem. 75 (4) (1999) 640–651.

[5] S. Swami, A.V. Krishnan, D. Feldman, 1 alpha,25-Dihydroxyvitamin D_3 down-regulates estrogen receptor abundance and suppresses estrogen actions in MCF-7 human breast cancer cells, Clin. Cancer Res. 6 (8) (2000) 3371–3379.

[6] M. Simboli-Campbell, C.J. Narvaez, K. van Weelden, M. Tenniswood, J. Welsh, Comparative effects of $1,25(OH)_2D_3$ and EB1089 on cell cycle kinetics and apoptosis in MCF-7 breast cancer cells, Breast Cancer Res. Treat. 42 (1) (1997) 31–41.

[7] E. Elstner, M. Linker-Israeli, J. Said, T. Umiel, S. de Vos, I.P. Shintaku, D. Heber, L. Binderup, M. Uskokovic, H.P. Koeffler, 20-epi-Vitamin D_3 analogues: a novel class of potent inhibitors of proliferation and inducers of differentiation of human breast cancer cell lines, Cancer Res. 55 (13) (1995) 2822–2830.

[8] J. Abe, T. Nakano, Y. Nishii, T. Matsumoto, E. Ogata, K. Ikeda, A novel Vitamin D_3 analog, 22-oxa-1,25 dihydroxyvitamin D_3 inhibits the growth of human breast cancer cells in vitro and in vivo without causing hypercalcemia, Endocrinology 129 (1991) 832–837.

[9] J. Akhter, X. Chen, P. Bowrey, E.J. Bolton, D.L. Morris, Vitamin D_3 analog, EB1089, inhibits growth of subcutaneous xenografts of the human colon cancer cell line, LoVo, in a nude mouse model, Dis. Colon Rectum 40 (3) (1997) 317–321.

[10] S.E. Blutt, T.C. Polek, L.V. Stewart, M.W. Kattan, N.L. Weigel, A calcitriol analogue, EB1089, inhibits the growth of LNCaP tumors in nude mice, Cancer Res. 60 (4) (2000) 779–782.

[11] C.M. Hansen, P.H. Maenpaa, EB1089, a novel Vitamin D analog with strong antiproliferative and differentiation-inducing effects on target cells, Biochem. Pharmacol. 54 (11) (1997) 1173–1179.

[12] S.Y. James, A.G. Mackay, K.W. Colston, Effects of 1,25 dihydroxyvitamin D_3 and its analogues on induction of apoptosis in breast cancer cells, J. Steroid Biochem. Mol. Biol. 58 (4) (1996) 395–401.

[13] S.Y. James, E. Mercer, M. Brady, L. Binderup, K.W. Colston, EB1089, a synthetic analogue of Vitamin D, induces apoptosis in breast cancer cells in vivo and in vitro, Br. J. Pharmacol. 125 (5) (1998) 953–962.

[14] K. VanWeelden, L. Flanagan, L. Binderup, M. Tenniswood, J. Welsh, Apoptotic regression of MCF-7 xenografts in nude mice treated with the Vitamin D_3 analog, EB1089, Endocrinology 139 (4) (1998) 2102–2110.

[15] L. Verlinden, A. Verstuyf, M. Van Camp, S. Marcelis, K. Sabbe, X.Y. Zhao, P. De Clercq, M. Vandewalle, R. Bouillon, Two novel 14-epi-analogues of 1,25-dihydroxyvitamin D_3 inhibit the growth of human breast cancer cells in vitro and in vivo, Cancer Res. 60 (10) (2000) 2673–2679.

[16] L. Verlinden, A. Verstuyf, R. Convents, S. Marcelis, M. Van Camp, R. Bouillon, Action of $1,25(OH)_2D_3$ on the cell cycle genes, cyclin D1, p21 and p27 in MCF-7 cells, Mol. Cell Endocrinol. 142 (1–2) (1998) 57–65.

[17] G. Wu, R.S. Fan, W. Li, T.C. Ko, M.G. Brattain, Modulation of cell cycle control by Vitamin D_3 and its analogue, EB1089, in human breast cancer cells, Oncogene 15 (13) (1997) 1555–1563.

[18] C.J. Narvaez, J. Welsh, Role of mitochondria and caspases in Vitamin D-mediated apoptosis of MCF-7 breast cancer cells, J. Biol. Chem. 276 (12) (2001) 9101–9107.

[19] T. Gulliford, J. English, K.W. Colston, P. Menday, S. Moller, R.C. Coombes, A phase I study of the Vitamin D analogue EB1089 in patients with advanced breast and colorectal cancer, Br. J. Cancer 78 (1) (1998) 6–13.

[20] B.L. Lokeshwar, G.G. Schwartz, M.G. Selzer, K.L. Burnstein, S.H. Zhuang, N.L. Block, L. Binderup, Inhibition of prostate cancer metastasis in vivo: a comparison of 1,23-dihydroxyvitamin D (calcitriol) and EB1089, Cancer Epidemiol. Biomarkers Prev. 8 (3) (1999) 241–248.

[21] K. El Abdaimi, N. Dion, V. Papavasiliou, P.E. Cardinal, L. Binderup, D. Goltzman, L.G. Ste-Marie, R. Kremer, The Vitamin D analogue

EB1089 prevents skeletal metastasis and prolongs survival time in nude mice transplanted with human breast cancer cells, Cancer Res. 60 (16) (2000) 4412–4418.
[22] D.J. Mantell, P.E. Owens, N.J. Bundred, E.B. Mawer, A.E. Canfield, 1 alpha,25-Dihydroxyvitamin D(3) inhibits angiogenesis in vitro and in vivo, Circ. Res. 87 (3) (2000) 214–220.
[23] H. Matsumoto, Y. Iino, Y. Koibuchi, T. Andoh, Y. Horii, H. Takei, J. Horiguchi, M. Maemura, T. Yokoe, Y. Morishita, Antitumor effect of 22-oxacalcitriol on estrogen receptor-negative MDA-MB-231 tumors in athymic mice, Oncol. Rep. 6 (2) (1999) 349–352.
[24] L. Flanagan, K. Van Weelden, C. Ammerman, S.P. Ethier, J. Welsh, SUM-159PT cells: a novel estrogen independent human breast cancer model system, Breast Cancer Res. Treat. 58 (3) (1999) 193–204.
[25] C.J. Narvaez, K. Vanweelden, I. Byrne, J. Welsh, Characterization of a Vitamin D_3-resistant MCF-7 cell line, Endocrinology 137 (2) (1996) 400–409.
[26] D.R. Green, J.C. Reed, Mitochondria and apoptosis, Science 281 (5381) (1998) 1309–1312.
[27] M. Crompton, The mitochondrial permeability transition pore and its role in cell death, Biochem. J. 341 (2) (1999) 233–249.
[28] R.R. Buras, L.M. Schumaker, F. Davoodi, R.V. Brenner, M. Shabahang, Vitamin D receptors in breast cancer, Breast Cancer Res. Treat. 31 (1994) 191–202.
[29] N.C. Arbour, J.M. Prahl, H.F. DeLuca, Stabilization of the Vitamin D receptor in rat osteosarcoma cells through the action of 1,25-dihydroxyvitamin D_3, Mol. Endocrinol. 7 (10) (1993) 1307–1312.
[30] I.M. Byrne, L. Flanagan, M.P. Tenniswood, J. Welsh, Identification of a hormone-responsive promoter immediately upstream of exon 1c in the human Vitamin D receptor gene, Endocrinology 141 (8) (2000) 2829–2836.
[31] A. Stoica, M. Saceda, A. Fakhro, H.B. Solomon, B.D. Fenster, M.B. Martin, Regulation of estrogen receptor-alpha gene expression by 1,25-dihydroxyvitamin D in MCF-7 cells, J. Cell Biochem. 75 (4) (1999) 640–651.
[32] S.Y. James, A.G. Mackay, L. Binderup, K.W. Colston, Effects of a new synthetic Vitamin D analogue, EB1089, on the oestrogen-responsive growth of human breast cancer cells, J. Endocrinol. 141 (3) (1994) 555–563.
[33] C.M. Hansen, T.L. Frandsen, N. Brunner, L. Binderup, 1 alpha,25-Dihydroxyvitamin D_3 inhibits the invasive potential of human breast cancer cells in vitro, Clin. Exp. Metastasis 12 (3) (1994) 195–202.
[34] J. Abe-Hashimoto, T. Kikuchi, T. Matsumoto, Y. Nishii, E. Ogata, K. Ikeda, Antitumor effect of 22-oxa-calcitriol, a noncalcemic analogue of calcitriol, in athymic mice implanted with human breast carcinoma and its synergism with tamoxifen, Cancer Res. 53 (1993) 2534–2537.
[35] K.W. Colston, A.G. Mackay, S.Y. James, L. Binderup, S. Chander, R.C. Coombes, EB1089: a new Vitamin D analogue that inhibits the growth of breast cancer cells in vivo and in vitro, Biochem. Pharmacol. 44 (12) (1992) 2273–2280.
[36] J.E. Price, A. Polyzos, R.D. Zhang, L.M. Daniels, Tumorigenicity and metastasis of human breast carcinoma cell lines in nude mice, Cancer Res. 50 (3) (1990) 717–721.
[37] J.E. Price, Metastasis from human breast cancer cell lines, Breast Cancer Res. Treat. 39 (1) (1996) 93–102.
[38] U. Berger, R.A. McClelland, P. Wilson, G.L. Greene, M.R. Haussler, J.W. Pike, K. Colston, D. Easton, R.C. Coombes, Immunocytochemical determination of estrogen receptor, progesterone receptor, and 1,25-$(OH)_2$-Vitamin D_3 receptor in breast cancer and relationship to prognosis, Cancer Res. 51 (1991) 239–244.